

Hypothesis testing at the extremes: fast and robust association for high-throughput data

Yi-Hui Zhou* and Fred A. Wright

*Bioinformatics Research Center and Department of Statistics
North Carolina State University
Cox Hall
2700 Stinson Dr.
Raleigh, NC 27695*

Abstract: A number of biomedical problems require performing many hypothesis tests, with an attendant need to apply stringent thresholds. Often the data take the form of a series of predictor vectors, each of which must be compared with a single response vector, perhaps with nuisance covariates. Parametric tests of association are often used, but can result in inaccurate type I error at the extreme thresholds, even for large sample sizes. Furthermore, standard two-sided testing can reduce power compared to the doubled p -value, due to asymmetry in the null distribution. Exact (permutation) testing is attractive, but can be computationally intensive and cumbersome. We present an approximation to exact association tests of trend that is accurate and fast enough for standard use in high-throughput settings, and can easily provide standard two-sided or doubled p -values. The approach is shown to be equivalent under permutation to likelihood ratio tests for the most commonly used generalized linear models. For linear regression, covariates are handled by working with covariate-residualized responses and predictors. For generalized linear models, stratified covariates can be handled in a manner similar to exact conditional testing. Simulations and examples illustrate the wide applicability of the approach.

Keywords and phrases: exact testing, density approximation, permutation.

1. Introduction

High dimensional datasets are now common in a variety of biomedical applications, arising from genomics or other high-throughput platforms. A standard question is whether a clinical or experimental variable (hereafter called the *response*) is related to any of a potentially large number of *predictors*. We use \mathbf{y} to denote the response vector of length n (random vector Y , observed elements y_j), and \mathbf{X} to denote the $m \times n$ matrix of predictors. Standard analysis often begins by testing for association of \mathbf{y} vs. each row \mathbf{x}_i of \mathbf{X} , i.e. computing a statistic $r_i = r(\mathbf{x}_i, \mathbf{y})$ for each hypothesis i . The most common corrections for multiple testing, such as Benjamini-Hochberg false discovery rate control, require only individual p -values for the m test statistics. Thus, at the level of a single hypothesis, the role of m is to determine the stringency of multiple testing. For modern

genomic datasets, m can reach 1 million or more, and individual p -values on the order of $\alpha = 10^{-7}$ may be required to declare significance. Standard parametric p -values may be highly inaccurate at these extremes, even for sample sizes $n > 1000$, if the data depart from parametric distributional assumptions.

Although the basic problem described here is familiar, current techniques often fail for extreme statistics, or are not designed for arbitrary data types. The researcher often resorts to parametric testing, even when the model is not considered quite appropriate, or may rely on central limit properties without a clear understanding of the limitations for finite samples. In genomics problems, such as SNP association testing involving contingency tables, the researcher may employ a hybrid approach in which most SNPs are tested parametrically, but those producing low cell counts are subjected to exact testing. Such two-step testing can be computationally intensive and cumbersome, and provides no guidance for situations in which the data are continuous or mixtures of discrete and continuous observations.

Our goal in this paper is to introduce a general trend testing procedure that is fast, provides accurate p -values simultaneously for all m hypotheses, and is largely distribution-free.

2. Exact testing and a summary of the approach

Exact testing is an attractive alternative to parametric testing, in which inference is performed on the observed \mathbf{y} and \mathbf{x}_i . In this discussion, i is arbitrary, and we suppress the subscript. We use $\pi = 1, \dots, n!$ to denote an index corresponding to each of the possible permutations, used as a subscript to represent re-ordering of a vector, with elements denoted $\pi[1], \dots, \pi[n]$. We use Π to denote a random permutation, producing the random statistic $r(\mathbf{x}, \mathbf{y}_\Pi)$.

The null hypothesis H_0 holds that the distributions generating \mathbf{x} and \mathbf{y} are independent, and we use X, Y to refer to the respective random variables. We assume that at least one of the distributions is exchangeable, so that the joint probability distribution of (say) the response is $P_Y(y_1, y_2, \dots, y_n) = P_Y(y_{\pi[1]}, y_{\pi[2]}, \dots, y_{\pi[n]})$ for each π (pg. 268 of Good [5]). Appendix A contains additional remarks on the assumptions underlying exact testing and perspectives for our specific context. The vectors \mathbf{x} and \mathbf{y} are fixed and observed, but the standard parametric tests rely on distributional assumptions for X and Y . Thus we will informally refer to the observed vectors as “discrete” or “continuous” according to the population assumptions, although the observed vectors are always discrete.

Throughout this paper, we use the statistic $r(\mathbf{x}, \mathbf{y}) = \sum_j x_j y_j$, which is sensitive to linear trend association. For discussion and plotting purposes, it is often convenient to center and scale \mathbf{x} and \mathbf{y} so that r is the Pearson correlation. As we show in Appendix B, most trend statistics of interest, including contingency table trend tests, t -tests, linear regression, and generalized linear model likelihood ratios, are permutationally equivalent to r .

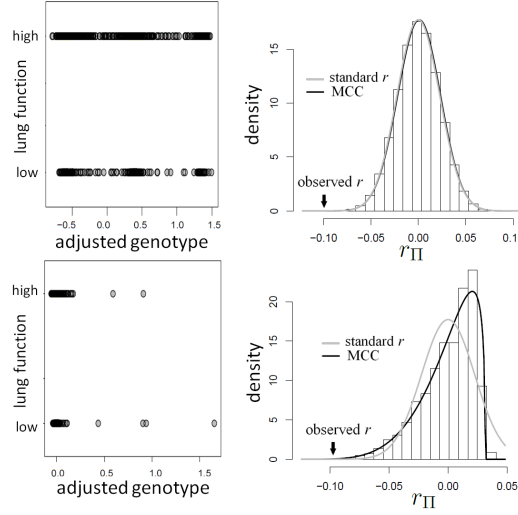


FIG 1. MCC for genotype association testing. Upper left: Data for SNP rs2956073. Although SNP genotypes were initially coded as 0, 1, 2, after covariate adjustment they appear as shown. Upper right: Histogram of r_{Π} , with standard r and MCC fitted densities. Lower left: SNP rs180784621, with a low minor allele frequency producing considerable skew in the adjusted genotypes. Lower right: Histogram of r_{Π} shows that MCC fits much better than standard r .

2.1. Summary of the approach

In this paper we introduce the *moment-corrected correlation* (MCC) method of testing. The basic idea of MCC is as follows – using moments of the observed \mathbf{x} and \mathbf{y} , we obtain the first four exact permutation moments of r_{Π} . We then apply a density approximation to fit the distribution, performed for the rows of matrix \mathbf{X} to simultaneously obtain p -values for all m hypotheses. MCC is “robust” in the sense that exact permutation moments are used, with two extra moments beyond the first two moments that are used in, e.g., a normal approximations to a statistic of interest.

3. A motivating example

We illustrate the concepts with an example from the genome-wide scan of Wright et al. Wright et al. [20], reporting association of $\sim 570,000$ SNPs with lung function in 1978 cystic fibrosis patients with the most common form of the disease. A significant association was reported on chromosome 11p, in the region between the genes *EHF* and *APIP*. To illustrate the effects of using skewed phenotype y , we use these data after covariate correction to consider a hypothetical follow-up regional search for associations to a binary indicator for extreme phenotype ($y = 1$ if the lung phenotype is above the 10th percentile, $y = 0$ otherwise).

With a highly skewed phenotype, these data are also emblematic of highly unbalanced case-control data, as might occur when abundant public data are used as controls Mukherjee et al. [14].

We performed logistic regression for phenotype vs. covariate-adjusted genotype for 3117 SNPs in a 1.5 Mb region containing the genes, and applied Benjamini-Hochberg q -value adjustment for the region. Two SNPs met regional significance at $q < 0.01$, rs2956073 (logistic Wald $p = 7.9 \times 10^{-6}$), and rs180784621 ($p = 1.8 \times 10^{-5}$). The sample size of $n = 1978$ would seem more than sufficient for analysis using large-sample approximations. However, histograms of the genotype-phenotype correlation coefficients (Figure 1) for 10^8 permutations for each SNP raises potential concerns for “standard” analysis of the second SNP (lower panels). Here the correlation distribution r_{Π} is strongly left-skewed, suggesting potential inaccuracy in p -values based on standard parametric approaches. Direct permutation, as shown in the figure, provides accurate p -values, but is computationally intensive (keeping in mind that the eventual application is to an entire matrix \mathbf{X}).

Overlaid on the histograms (Figure 1) in grey is the “standard r ” density $f(r) = B(\frac{1}{2}, \frac{1}{2}(n-2))^{-1} (1-r^2)^{\frac{n-4}{2}}, r \in (-1, 1)$ where $B(\cdot)$ is the beta function. This density is the unconditional distribution of r under H_0 if either X or Y is normally distributed Lehmann and Romano [10], and tests based on it are equivalent to t -testing based on simple linear regression or the two-sample equal-variance t , and similar to a Wald statistic from logistic regression.

The example provides a preview of the advantage of using MCC. For the top right panel, the histogram is closely approximated by the standard r density, as well as by MCC (black curve). However, for the lower right panel, MCC is much more accurate than standard r in approximating the histogram, with dramatic differences in the extreme tails. The reason for the improvement is that MCC uses the first four exact moments of r_{Π} to provide a density fit.

When the distribution of r_{Π} is skewed, more than one type of p -value might reasonably be used. Typical choices include p -values based on either extremity of $|r_{\Pi}|$, or by doubling the smaller of the two “tail” regions (Kulinskaya [8], see below). For the first SNP, these two p -values (based on extremity or tail-doubling) are nearly identical, but can be very different when the distribution of r_{Π} is skewed, as in the lower panels. Thus, in addition to accuracy of p -values, we must also consider the relative power obtained by the choice of p -value.

4. Trend statistics and p -values

4.1. r_{Π} and trend statistics are permutationally equivalent

Over permutations, r is one-to-one with most standard trend statistics, which are described in terms of distributional assumptions for X and Y . A list of such standard statistics is given below, and Appendix B provides citations and derivations for the permutationally equivalent property. Standard parametric tests/statistics include simple linear regression (X arbitrary, Y continuous), and

the two sample problem as a special case (X binary, Y continuous). For the latter we do not distinguish between equal-variance and unequal-variance testing, working directly with mean differences in the two samples under permutation. Categorical comparisons include the contingency table linear trend statistic (X ordinal, Y ordinal) Stokes and Koch [18], which includes the Cochran-Armitage statistic (X ordinal, Y binary) Armitage [1] and the chisquare and Fisher’s exact tests for 2×2 tables. If X or Y represent ranked values, the standard statistics include the Wilcoxon rank sum (X binary, Y ranked values), and the Spearman rank correlation (X ranked, Y ranked). Other statistics with the property include likelihood ratios or deviances for essentially all common two-variable generalized linear models (GLMs), when the permutations have been partitioned according to $\text{sign}(r)$. These GLMs include logistic and probit (X binary or continuous, Y binary), Poisson (X continuous or discrete, Y integer), and common overdispersion models.

For the standard statistics, it is thus sufficient to work directly with r_Π for testing against the null. There is no need to be concerned over differences among the statistics, or to perform computationally expensive maximum likelihood fitting, because the statistics are equivalent. Finally, we note that the use of correlation makes it obvious that the roles of \mathbf{x} and \mathbf{y} are interchangeable.

4.2. *P-values*

The observed r_{obs} can be compared to r_Π to obtain a two-sided p -value

$$p_{two} = Pr(|r_\Pi| \geq |r_{obs}|).$$

Alternatively, we might obtain left and right-tail p -values $p_{left} = Pr(r_\Pi \leq r_{obs})$, $p_{right} = Pr(r_\Pi \geq r_{obs})$, with “directional” $p_{directional} = \min(p_{left}, p_{right})$. The directional p -value is not a true p -value, as it uses the data to choose the favorable direction. However, simply doubling it produces a proper p -value,

$$p_{double} = 2 \times p_{directional}.$$

For skewed r_Π , p_{double} often has a power advantage over p_{two} , provided the investigator maintains equipoise in prior belief of positive vs. negative correlation between X and Y . Figure 2 shows the power for an illustrative model, with $Y = \beta X + \epsilon_Y$, $n = 50$, and significance level $\alpha = 10^{-5}$. 1000 simulations were performed, and 10^6 permutations performed for each simulation to obtain the two types of p -values. Two scenarios are shown: (i) $X \sim N(0, 1)$ and $\epsilon_Y \sim \exp(1)$ (exponential with mean 1, left panel), and (ii) $X \sim \exp(1)$, $\epsilon_Y \sim \exp(1)$ (right panel), with the power each $|\beta|$ value averaged over the power for the corresponding positive and negative β . Skew in r_Π requires that both \mathbf{x} and \mathbf{y} be skewed (Appendix C), and the random variable X is skewed only for scenario (ii). Accordingly, p_{double} and p_{two} are essentially identical in the left panel, while in the right panel, skew in r_Π provides an advantage to p_{double} .

The intuition behind the increased power of p_{double} comes from the fact that for a skewed r_Π , doubling the smaller of the two tail regions is typically smaller

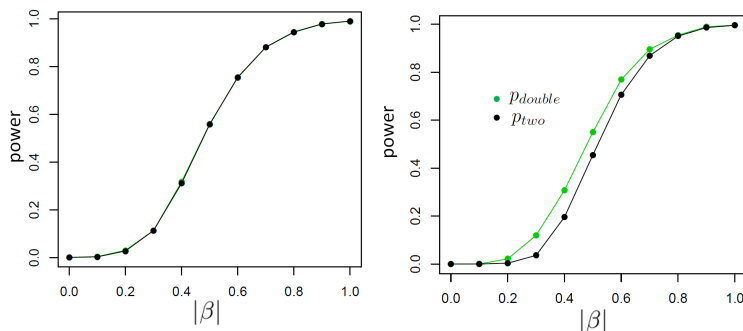


FIG 2. Left panel: with no skew in r_{Π} , p_{two} and p_{double} have the same power (black is overlaid over green). Right panel: when r_{Π} is skewed, p_{double} has a power advantage.

than the sum of the two tail regions used by p_{two} . Appendix D proves the increased power for local departures from the null, when approximating r_{Π} using a specific class of skewed densities. The historical use and properties of doubled p -values, as well as alternative constructions, are described in Kulinskaya [8].

The MCC approach described below is accurate for both p_{two} and p_{double} , but we primarily focus on p_{double} , and thus we evaluate MCC and standard parametric tests in terms of accuracy of $p_{directional}$, except where noted.

5. Computation, density fitting, and an improvement

MCC can be used for a large variety of linear and generalized linear models and for categorical tests of trend. A simple extension to MCC is also proposed to improve accuracy in the presence of modest outliers. Finally, we describe approaches to handle covariates. Several well-studied examples from the literature, not necessarily high throughput, are used to illustrate.

5.1. A density fit

The mean and variance of correlation r_{Π} are always 0 and $1/(n-1)$ Pitman [15]. The exact skewness and kurtosis are derived in Pitman [15] in terms of Fisher k -statistics. In Appendix C, to illustrate we recompute the kurtosis as a function of the moments of \mathbf{x} and \mathbf{y} . We use a re-scaled beta density to fit the distribution of r_{Π} (Appendix E) and compute correspondingly estimated p -values. If n is very small, or there are numerous tied values in \mathbf{x} and \mathbf{y} , accuracy of the density approximation will be slightly affected by tied instances in r_{Π} , and the approximation is often closer to the mid p -value, e.g. $\hat{p}_{right} \approx Pr(r_{\Pi} > r_{obs}) + \frac{1}{2}P(r_{\Pi} = r_{obs})$.

For simple linear models, such as $Y = \beta_0 + \beta_1 X + \epsilon_Y$, where the ϵ values are assumed drawn iid from an arbitrary density, MCC can be used to provide approximations to exact confidence intervals for β_1 , by inverting the test using

the MCC p -values for comparing \mathbf{x} to $\mathbf{y} - \beta_1 \mathbf{x}$ (the value of β_0 is immaterial in the correlation). Examples of these intervals are shown in the Appendix.

5.2. Computational cost

MCC requires several matrix operations performed on \mathbf{X} , involving computing element-wise powers (up to 4) followed by row summations, which are $O(mn)$ operations. Other operations are of lower order, so the overall order is $O(mn)$. To empirically demonstrate, we ran the R scripts using simulated data with $m = 2^a$, with $a \in \{10, 11, \dots, 18\}$ (i.e. m ranging from 1024 to 262,144), and $n = 2^b$, with $b \in \{9, \dots, 12\}$ (i.e. n ranging from 512 to 4096). The $9 \times 4 = 36$ scenarios were analyzed using a Xeon 2.65 GHz processor, and the largest scenario ($m = 262,144, n = 4096$) took 376 seconds. Computation for a genome-wide association scan with $m=1$ million markers and $n = 1000$ individuals takes a similar time (≈ 6 minutes). Appendix F shows the timing for all 36 scenarios, and the results of a model fit to the elapsed time. We note that computation of the observed r for all m features is itself an $O(mn)$ computation.

5.3. A one-step improvement to MCC

Extreme values in either \mathbf{x} or \mathbf{y} present a challenge for MCC, especially in smaller datasets, as these values have high influence and can even produce a multimodal r_Π distribution. Extensions of MCC using higher moments is possible, but cumbersome. A more direct approach is to condition on an influential observation, which we call the referent sample. Below, without loss of generality we can consider the referent sample to be sample 1. We have

$$\begin{aligned} r_\pi &= \sum_j x_j y_{\pi[j]} = x_1 y_{\pi[1]} + \sum_{j=2}^n x_j y_{\pi[j]} \\ &= x_1 y_{\pi[1]} + b_{0,\pi[1]} + b_{1,\pi[1]} r_{-\pi[1]}, \end{aligned}$$

where $r_{-\pi[1]}$ is the random correlation between the \mathbf{x} and \mathbf{y} vectors after removal of the x_1 and $y_{\pi[1]}$ elements (Appendix G), and $b_{0,\pi[1]}, b_{1,\pi[1]}$ are normalization constants. The n possible $y_{\pi[1]}$ values each generate $(n-1)!$ values of $r_{-\pi[1]}$. We denote the beta density approximation applied to each of the n possibilities as $f(r|x_1, y_{\pi[1]})$, finally obtaining the approximation $g(r) = \frac{1}{n} \sum_{\pi[1]=1}^n f(r|x_1, y_{\pi[1]})$. We refer to this one-step approximation as MCC_1 . The motivation behind MCC_1 is that the most extreme values of r_Π must contain pairings of extreme \mathbf{x} and \mathbf{y} elements, and so the benefit is often seen in the tail regions.

In order to avoid arbitrariness in the choice of “extreme” value, we can also consider each of the n observations in turn as the referent sample and average over the result (which we call $\text{MCC}_{1,\text{all}}$). Applying $\text{MCC}_{1,\text{all}}$ adds an additional factor n^2 in computation compared to MCC, and thus in practice we apply it only to features for which the MCC p -value is many orders of magnitude smaller than the standard parametric p -value.

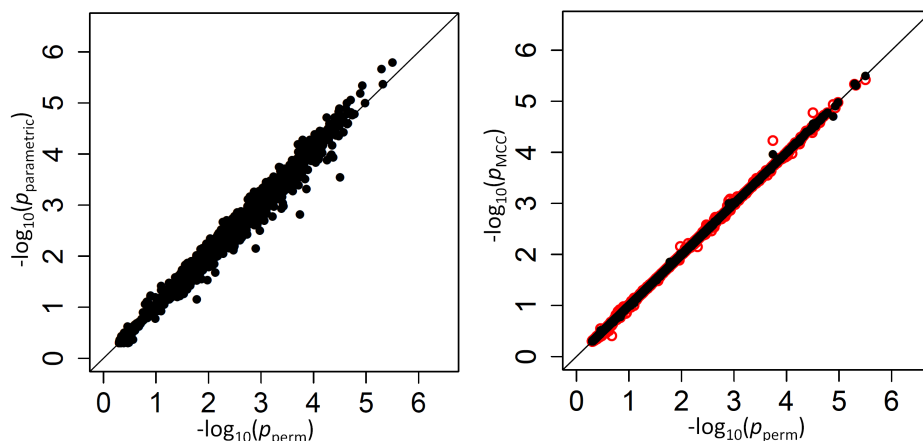


FIG 3. Performance of MCC for the breast cancer survival data Left panel: Directional p -values using a two-sample t test vs. a large number of permutations. Right panel: p -values using MCC vs. permutations (red), and using MCC_1 (black).

5.4. Examples

As a high throughput example we use a breast cancer gene expression dataset, consisting of 236 samples on the Affy U133A expression array, with a disease survival quantitative phenotype Miller et al. [12]. Figure 3 (left panel) shows the results of comparing directional p -values based on the t -statistic from standard linear regression to those of actual permutation. The permutation was conducted in two stages, with 10^6 permutations for each gene in stage 1, and for any gene with a permutation $p < 0.05$ in stage 1, another 10^8 permutations were performed. The right panel shows the analogous results for MCC (red, analyzed in 1 sec for all genes) and MCC_1 (black, analyzed in 1 minute). Here for MCC_1 the sample with the most outlying survival phenotype value (judged by absolute deviation from the median) was used as the referent sample. Clearly both versions of MCC considerably outperform regression, and here MCC_1 provides a modest improvement over MCC.

Another example, in which both \mathbf{x} and \mathbf{y} are discrete, is given by the dataset published by Takei et al. [19], which describes association of Alzheimer disease with several SNPs in the *APOE* region. Although only a few SNPs were investigated, the approaches are identical to those used in genome scans involving up to millions of SNPs. The published analyses used the Cochran-Armitage trend statistic, which is compared to a standard normal. Exact p -values are feasible to compute in this instance. In these data, the case-control ratios are close enough to a 1:1 ratio that the trend statistic performs well, as do most other methods (see Figure 4). An exception is the Wald logistic p -value, which is the default logistic regression approach in genetic analysis tools such as PLINK Purcell et al.

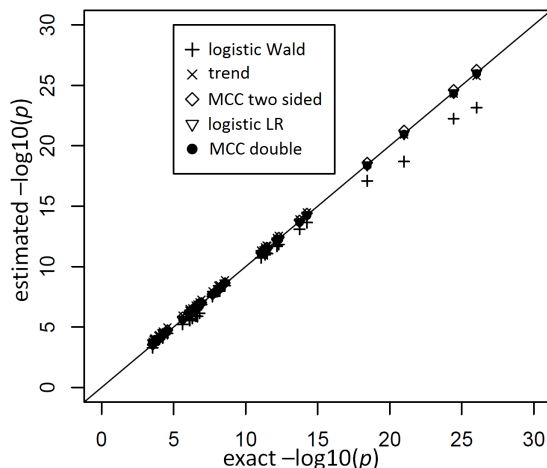


FIG 4. Results for the analysis of 35 SNPs in the APOE region vs. late-onset Alzheimer disease in Japanese, from Takei et al. (Takei et al. [19])

[16], and can depart noticeably from the exact result for the most extreme SNPs. The figure shows two-sided p -values, but the pattern for directional p -values is similar. For modern genomic analyses with over 1 million markers, computing logistic regression likelihood ratios can be time-consuming, as are exact analyses. Moreover, exact methods are not available (except via permutation) for imputed markers, which assume fractional “dosage” values Li et al. [11], while MCC is still applicable.

A more detailed examination of r_{Π} for a significant gene in an expression study is shown in Appendix H, focusing on the behavior in tail regions.

Another proposed alternative to direct permutation is to use saddlepoint approximations Robinson [17], Booth and Butler [2], which have been examined in considerable detail for a few relatively small datasets. In Appendix I, we illustrate the analysis of two datasets from Lehmann Lehmann [9]. The datasets show that MCC is at least as accurate as saddlepoint approximations, and far easier to implement.

5.5. Covariate control by residualization

Although association testing of two variables is simple, it has wide application for screening purposes. This utility can be further extended to accommodate covariates. Covariate control within our framework is most straightforward when linear regression models are applicable for both X and Y . In such instances, we assume $Y = \beta_0 + \beta_1 X + \beta_2 Z + \epsilon_Y$, where Z is a vector (or matrix) of covariates, β_2 a covariate coefficient (or vector of coefficients), and the ϵ_Y values are drawn independently from an arbitrary density. The correspondence between Z and X

may be similarly modeled $X = \alpha_0 + \alpha_1 Z + \epsilon_X$. Under the null hypothesis $\beta_1 = 0$, $Y - \beta_2 Z$ is independent of $X - \alpha_1 Z$. Thus an obvious testing approach is to use permutation or MCC to compare $\mathbf{y}_z = \mathbf{y} - \hat{\beta}_{10} - \hat{\beta}_2 \mathbf{Z}$ to $\mathbf{x}_z = \mathbf{x} - \hat{\alpha}_0 - \hat{\alpha}_1 Z$, where the parameter estimates are obtained via linear regression Kennedy and Cade [7]. The residualized quantities \mathbf{x}_z and \mathbf{y}_z are technically no longer exchangeable, even under the null $\beta_1 = 0$, due to error in the estimation of β_2 and α_1 . However, for large sample sizes and few covariates, the impact of this source of error becomes negligible, especially in comparison to the inaccuracies produced by reliance on standard parametric p -values.

To evaluate the effectiveness of residualized covariate control, for a fixed dataset we can compare the distribution of the true $\epsilon_{\mathbf{x}}, \epsilon_{\mathbf{y}, \Pi}$ to that of $r(\mathbf{x}_z, \mathbf{y}_{z, \Pi})$, where $\mathbf{y}_{z, \pi}$ denotes the π -permutation of \mathbf{y}_z . An example of this kind of covariate control is shown in later simulated datasets.

5.6. Covariate control by stratification

For generalized linear models under permutation, covariate control is not as straightforward, as there are no precisely analogous results to the partial correlations described above (or even quantities such as $\epsilon_{\mathbf{y}}$). We consider a discrete covariate vector $\mathbf{z} \in (1, \dots, K)$ and define J_k as the indexes for the observations assuming the k th covariate value, i.e. $J_k = \{j : \mathbf{z} = k\}$. Denoting the within-stratum sum $A_k = \sum_{j \in J_k} x_j y_j$, we have $A = \sum_{j=1}^n x_j y_j = \sum_{k=1}^K A_k$. The moments of A are described in Appendix J. For this subsection we use different notation (A instead of r) because, in the stratified setting, there is no algebraic advantage to rescaling \mathbf{x} and \mathbf{y} to be equivalent to the Pearson correlation. However, A is used and interpreted essentially in the same manner as r . The key to stratified covariate control is to perform permutation between \mathbf{x} and \mathbf{y} *within* strata, so there are $\prod_{k=1}^K (n_k!)$ total permutations. We note that this stratified approach is similar to the principle underlying exact conditional logistic regression Cox and Snell [4], Corcoran et al. [3]. The moments of each A_k under permutation are obtained using the same approach described earlier for r_{Π} , and because the strata are permuted independently, the moments for stratified A_{Π} are straightforward. We note that stratification does not change the computational complexity. For the 36 scenarios described in the earlier timing subsection, stratification by a 32-level covariate in fact reduced the computational time approximately 22% when averaged over the scenarios, due to some savings in lower-order computation.

Figure 5 shows the result of applying MCC to the data from Breslow and Day (1980) on binary outcome data for endometrial cancer for 63 matched pairs, with gall bladder disease as the predictor and the matched pairs used to form covariate strata. This is an extreme instance with 63 strata. The figure shows the close fit of MCC to the data, although due to discrete outcomes on the integers, a continuity correction is necessary for accurate p -values. For $A_{\text{observed}} = 14$, the doubled p -value is obtained by computing MCC after applying a 0.5 offset, resulting in $p_{\text{double}} = 0.1007$. The exact p -value obtained from 10^7 permutations

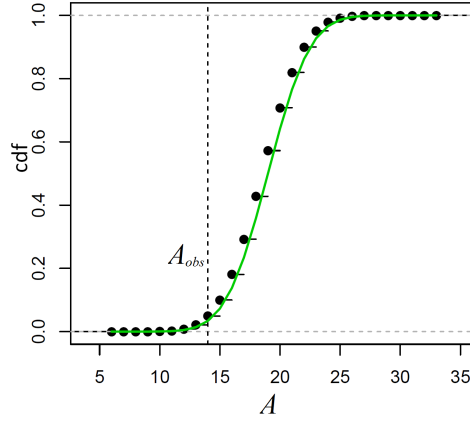


FIG 5. The distribution of A for the endometrial cancer data of Breslow and Day (1980), with gall bladder disease as a predictor and matched case-control pairs. The empirical cdf is based on 10^7 stratified permutations, while the green curve is based on the MCC fit.

is 0.0996.

6. Additional simulated datasets

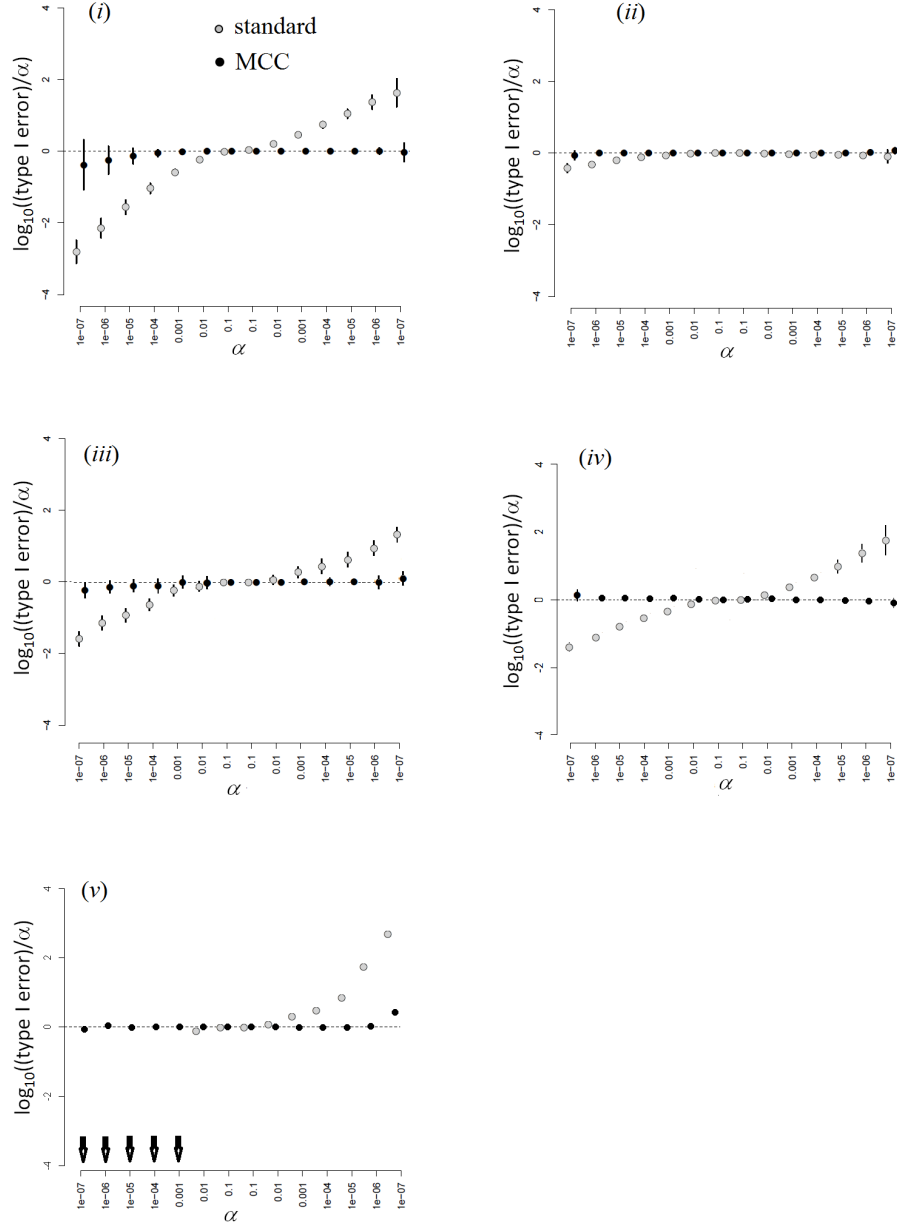
We now consider additional simulations involve discrete outcomes or covariates, using “ \sim ” to signify the distribution from which values are drawn. We perform 10^8 permutations, for each of $n = 500, 1000, 2000$, performed for 10 simulations. The relatively large sample sizes are intended to match large-scale ‘omics datasets, where large sample sizes are necessary to achieve stringent significance thresholds.

(i) *Two-sample mixed discrete/continuous*: we consider X drawn as a mixture of 50% zeros and the remainder drawn from a χ_1^2 density, $Y \sim \text{Binom}(1, 0.2)$. One “standard” approach is the two-sample unequal variance t -test, although some investigators might be uncomfortable with the large number of zero values.

(ii) *Ranks of mixed discrete/continuous*: we consider an initial X' drawn as a mixture with $X' = 0$ with probability 0.2, $X' = 3.0$ with probability 0.1, and the remainder drawn from a χ_1^2 density, $Y \sim \text{Binom}(1, 0.2)$. Then for observed \mathbf{x}' , we use the ranks $\mathbf{x} = \text{rank}(\mathbf{x}')$. The standard approach is the two-sample Wilcoxon rank sum test, but due to the large number of ties, the standard distributional approximation for the Wilcoxon may not be accurate.

(iii) *Case/Control*: $X \sim \text{Binom}(2, 0.1)$, $Y \sim \text{Binom}(1, 0.2)$, which mimics the outcome of a unbalanced case-control study in which \mathbf{y} is an indicator for case status, and \mathbf{x} a discrete covariate such as SNP genotype. Standard approaches are the Cochran-Armitage trend test (shown here) or logistic regression.

(iv) *Continuous with continuous covariates*: To illustrate the effect of continuous covariate control, we simulated $\epsilon_X \sim \exp(1)$, $\epsilon_Y \sim \exp(1)$, with true models

FIG 6. Simulations with $n=500$, scenarios (i)-(v).

$Y = Z_1 + \epsilon_Y$, $X = 2Z_1 + \epsilon_X$. The covariates $Z_1 \sim N(0, 1)$ and $Z_2 \sim \exp(1)$ were fitted to the data, although only Z_1 was correlated with X and Y . The standard approach is linear regression.

(v) *Discrete with a stratified covariate*: We first simulated covariate $Z \sim \text{Binom}(1, 0.5)$, and then $X \sim \text{Binom}(2, 0.02 + 0.16Z)$, $Y \sim \text{Binom}(1, 0.04 + 0.32Z)$. Marginally, this is similar to (iii), except that X and Y have removable correlation induced by Z . The standard approach is logistic regression, with the effect of Z modeled as an additive covariate, which is correct under H_0 .

Figure 6 and Supplementary Figures 4-5 show the performance of directional p under the various scenarios. Performance is described in terms of $\log_{10}((\text{true type I error})/\alpha)$, where the true type I error is the probability that $p_{\text{directional}} \leq \alpha$ for each of the 10 simulations, and the values are shown as mean \pm 1 standard deviation. For scenarios (i), (iii), (iv), and (v), both X and Y are skewed, and the standard approaches are highly anticonservative in the right tail and conservative in the left tail (see Figure 6). In fact, for scenario (v), the standard left directional p -values are often unable to achieve sufficiently small values in order to be rejected. The performance of standard approaches is particularly poor for $n = 500$, but the performance remains poor even for $n = 2000$. MCC is much more accurate, down to $\alpha = 10^{-7}$. The standard approach for scenario (ii) is only modestly conservative in the left tail, which we attribute to the use of ranks, although due to ties some skew remains.

In summary, the standard approaches often have difficulty with type I error control, if both X and Y are skewed. However, MCC is well-behaved across all the scenarios. If the direction of skew were reversed for either X or Y , the patterns would change and the conservativeness would appear on the right.

7. An RNA-Seq example

As a final example, incorporating several of the aspects described above, we consider the RNA-Seq expression data of Montgomery et al. [13] from $n = 42$ HapMap CEU cell lines, with ranked IC_{50} values from exposure to etoposide Huang et al. [6] used as a response \mathbf{y} . For these samples, $m = 30,009$ genes which vary across the samples were used. We applied the residualization approach as described earlier, with sex as a stratified covariate. The RNA-Seq data were originally based on integer counts, which were then normalized as described in Zhou et al. [21] and covariate-residualized. We applied $\text{MCC}_{1,\text{all}}$ to the data for all features, requiring 25 minutes on the desktop PC used earlier for timing comparisons.

Figure 7 (top panels) shows the results for the most significant gene as determined by MCC, although not genome-wide significant (empirical $p_{\text{double}} = 7.4 \times 10^{-5}$ based on 10^8 permutations, $\text{MCC}_{1,\text{all}} p_{\text{double}} = 9.5 \times 10^{-5}$). The lower panels show an example gene that is not significant, but for which the distribution is highly multimodal, due to the presence of extreme count values in \mathbf{X}_i . Nonetheless, $\text{MCC}_{1,\text{all}}$ can effectively fit the density, by conditioning on the outlier.

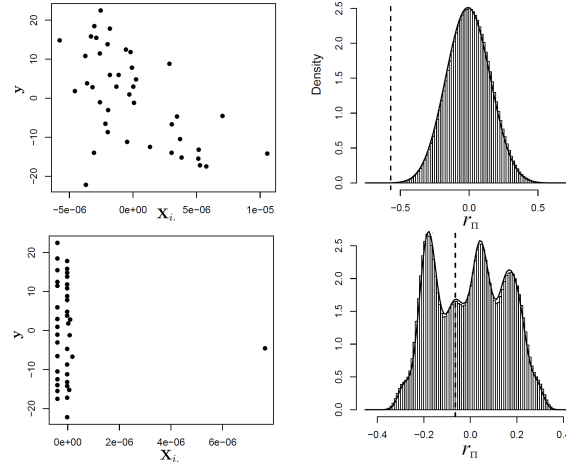


FIG 7. Residualized y vs. x_i , and null permutation histograms for the gene *TEAD4* (upper panels) and *AGT* (lower panels). The fitted $MCC_{1,all}$ densities are overlaid on the histograms, and the observed r_{obs} shown as a dashed line.

8. DISCUSSION

We have described a coherent and fast approach to perform trend testing of a single vector vs. all rows of a matrix, which is a canonical testing problem arising in genomics and other high-throughput applications. The approach largely eliminates the need to be concerned over the appropriate choice of trend statistic, or whether parametric testing can be justified for the data at hand. In specific settings, such as genotype association testing, concern over the minor allele frequencies often leads investigators to perform exact testing for a subset of markers. We clarify that the primary difficulty arises when both \mathbf{x} and \mathbf{y} are skewed, but the effects of the fourth moments may also be noticeable for extreme testing thresholds. For standard case-control studies with samples accrued in a 1:1 ratio, skewness may not be severe. However, for the analysis of binary secondary traits, the case:control ratio may depart from 1:1, and thus \mathbf{y} may be highly skewed. In addition, the expense of sequence-based genotyping has increased interest in using shared or common sets of controls, which could then be much larger than the number of cases.

A possible alternative approach is to simply transform \mathbf{x} and/or \mathbf{y} (e.g. to match quantiles of a normal density) so that standard approximations fit well. Although this approach may provide correct type I error, it may also distort the interpretability of a meaningful trait or phenotype. In addition, for discrete data, such as those used in case-control genetic association studies, no such transformation may be feasible. We also note that it is rare for such transformations to be considered prior to fitting generalized linear models, and thus our methodology remains highly relevant.

We note that the standard density approximation is intended for unconditional inference, i.e. not conditioning on the observed \mathbf{x} and \mathbf{y} . Thus it is in some sense unfair to expect a close correspondence to the permutation distribution, which is inherently conditional on the data. However, as we show below, if the densities of X and Y are skewed, standard parametric p -values tend to be inaccurate *on average*, in a manner that is largely reflected in comparisons such as shown in Figure 1.

9. Acknowledgments

Supported in part by the Gillings Statistical Genomics Innovation Lab, EPA RD83382501, NCI P01CA142538, NIEHS P30ES010126, P42ES005948 and HL068890. We thank Dr. Alan Agresti for pointing out the relevance of the Hauk and Donner 1977 paper described in the Appendix. We gratefully acknowledge the CF patients, the Cystic Fibrosis Foundation, the UNC Genetic Modier Study, and the Canadian Consortium for Cystic Fibrosis Genetic Studies, funded in part by Cystic Fibrosis Canada and by Genome Canada through the Ontario Genomics Institute per research agreement 2004-OGI-3-05, with the Ontario Research Fund-Research Excellence Program.

References

- [1] P. Armitage. Tests for linear trends in proportions and frequencies. *Biometrics*, 11(3):375–386, 1955.
- [2] J. G. Booth and R. W. Butler. Randomization distributions and saddlepoint approximations in generalized linear models. *Biometrika*, 77-4: 787–96, 1990.
- [3] C. Corcoran, C. Mehta, N. Patel, and P. Senchaudhuri. Computational tools for exact conditional logistic regression. *Statistics in Medicine*, 20 (17-18):2723–2739, 2001.
- [4] D. R. Cox and E. J. Snell. *Analysis of Binary Data*. Boca Raton: Chapman and Hall, 1989.
- [5] P. I. Good. *Permutation, Parametric, and Bootstrap Tests of Hypotheses*. Springer, 2005.
- [6] S. T. Huang, S. Duan, W. K. Bleibel, E. O. Kistner, W. Zhang, T. A. Clark, T. X. Chen, A. C. Schweitzer, J. E. Blume, N. J. Cox, and M. E. Dolan. A genome-wide approach to identify genetic variants that contribute to etoposide-induced cytotoxicity. *PNAS*, 104(23)(9758-9763), 2007.
- [7] P. E. Kennedy and B. S. Cade. Randomization tests for multiple regression. *Communications in Statistics - Simulation and Computation*, 25:4:923–936, 1996.
- [8] E. Kulinskaya. On two-sided P-values for nonsymmetric distributions. *Arxiv*, (0810:2124), 2008.
- [9] E. L. Lehmann. *Nonparametrics: Statistical Methods Based on Ranks*. San Francisco: Holden-Day, 1975.

- [10] E. L. Lehmann and J. P. Romano. *Testing Statistical Hypotheses*. Springer, 2005.
- [11] Y. Li, C. J. Willer, J. Ding, P. Scheet, and G. R. Abecasis. MaCH: using sequence and genotype data to estimate haplotypes and unobserved genotypes. *American Journal of Human Genetics*, 34(8):816–834, 2010.
- [12] L. D. Miller, J. Smeds, J. George, V. B. Vega, L. Vergara, A. Ploner, Y. Pawitan, P. Hall, S. Klaar, E. T. Liu, and J. Bergh. An expression signature for p53 status in human breast cancer predicts mutation status, transcriptional effects, and patient survival. *PNAS*, 102(38)(13550-5), 2005.
- [13] S. B. Montgomery, M. Sammeth, M. Gutierrez-Arcelus, R. P. Lach, C. Ingle, J. Nisbett, R. Guigo, and E. T. Dermitzakis. Transcriptome genetics using second generation sequencing in a Caucasian population. *Nature*, 464(7289)(773-777), 2010.
- [14] S. Mukherjee, J. Simon, S. Bayuga, E. Ludwig, S. Yoo, I. Orlow, A. Viale, K. Offit, R. C. Kurtz, S. H. Olson, et al. Including additional controls from public databases improves the power of a genome-wide association study. *Human heredity*, 72(1):21–34, 2011.
- [15] E. J. Pitman. Significance tests which may be applied to samples from any populations: Ii. the correlation coefficient test. *Suppl. J. R. Statist. Soc.*, 4.
- [16] S. Purcell, B. Neale, K. Todd-Brown, L. Thomas, M. A. Ferreira, J. Bender, D. Maller, P. Sklar, P. I. de Bakker, M. J. Daly, and P. C. Sham. PLINK: a tool set for whole-genome association and population-based linkage analyses. *American Journal of Human Genetics*, 81(3):559–75, 2007.
- [17] J. Robinson. Saddlepoint Approximations for Permutation Tests and Confidence Intervals. *Journal of the Royal Statistical Society*, 44(1)(91-101), 1982.
- [18] D. C. S. Stokes, M. E. and G. G. Koch. Categorical Data Analysis Using the SAS System. *SAS Institute Inc*, 2000.
- [19] N. Takei, A. Miyashita, T. Tsukie, H. Arai, T. Asada, M. Imagawa, M. Shoji, S. Higuchi, K. Urakami, H. Kimura, A. Kakita, H. Takahashi, S. Tsuji, I. Kanazawa, Y. Ihara, S. Odani, and R. Kuwano. Genetic association study on in and around the APOE in late-onset Alzheimer disease in Japanese. *Genomics*, 93(5)(441-8), 2009.
- [20] F. A. Wright, L. J. Strug, V. K. Doshi, C. W. Commander, S. M. Blackman, L. Sun, Y. Berthiaume, D. Cutler, A. Cojocaru, J. M. Collaco, et al. Genome-wide association and linkage identify modifier loci of lung disease severity in cystic fibrosis at 11p13 and 20q13. 2. *Nature Genetics*, 43(6): 539–546, 2011.
- [21] Y. H. Zhou, K. Xia, and F. A. Wright. A powerful and flexible approach to the analysis of RNA sequence count data. *Bioinformatics*, 27(19)(2672-8), 2011.

Hypothesis testing at the extremes: fast and robust association for high-throughput data

Yi-Hui Zhou* and Fred A. Wright

*Bioinformatics Research Center and Department of Statistics
North Carolina State University
Cox Hall
2700 Stinson Dr.
Raleigh, NC 27695*

Keywords and phrases: exact testing, density approximation, permutation.

1. Appendix A

We assume exchangeability, but in many applications we expect that the elements of (say) \mathbf{y} are in fact independent. However, the weaker exchangeability requirement is useful to clarify that various forms of pre-treating the data, such as normalization techniques, do not invalidate permutation testing. The same comment applies to normalization of \mathbf{X} , provided that \mathbf{X} and \mathbf{y} are normalized separately. Conditioned on the observed \mathbf{x} and \mathbf{y} , under H_0 each of the $n!$ permuted versions of \mathbf{y} is equally likely to have arisen in relation to the elements of \mathbf{x} , and these permutations are the population upon which inference is based. We use Π to denote a random permutation, drawn uniformly from these possibilities. The permutation in turn produces the random statistic $r(\mathbf{x}, \mathbf{y}_\Pi)$, upon which an exact p -value P_Π is based.

A primary advantage to exact testing is the distribution-free property. If X and Y have continuous densities, r_Π will assume $n!$ unique values, and a p -value (e.g., p_{left}) will be rank-uniform, assuming of the values $\{1/n!, 2/n!, \dots, 1\}$ each with probability $1/n!$. This property ensures approximate validity, $Pr(P_\Pi \leq \alpha | data) \approx \alpha$, and that the p -value is also valid unconditionally, so $Pr(P_\Pi \leq \alpha) \approx \alpha$. Exact testing methods are familiar to many practitioners, but are often discussed in the more limited context of rank methods or discrete data. Thus we make a few additional remarks to clarify our treatment here.

- Exchangeability of *either* X or Y is sufficient. One practical consequence is that the response vector may be fixed by design, and need not be thought of as “random.”
- The number of unique $r(\mathbf{x}, \mathbf{y}_\Pi)$ outcomes may be much smaller than $n!$, depending on the choice of statistic, or tied values in \mathbf{x} or \mathbf{y} . As an extreme example, consider binary \mathbf{x} and \mathbf{y} , and Fisher’s exact test of the corresponding 2×2 table. Fisher’s p -value is typically computed using

summations of hypergeometric outcome probabilities, thus avoiding enumeration of all $n!$ possibilities. However, complete $n!$ enumeration would produce the same p -value.

- A large literature has considered the conservativeness of exact testing (e.g., Agresti and Coull [2]), due to tied values in \mathbf{x} and \mathbf{y} producing tied values in $r(\mathbf{x}, \mathbf{y}_\Pi)$. Although such conservativeness is an important consideration for small sample sizes, for large sample sizes this phenomenon is of lesser importance.
- Even a slight skew in $r(\mathbf{x}, \mathbf{y}_\Pi)$ can, for extreme values of the statistic, produce a marked departure in p -values computed using permutation vs. standard parametric approaches. This matter has received little attention, which we attribute primarily to the historical focus on $\alpha = 0.05$, for which the differences between permutation and parametric analysis are often minimal.

2. Appendix B: citations and derivations for the permutationally equivalent property

Adapting the definition in Pesarin and Salmaso [10] (pg. 48) to our setting, statistics r and s are defined to be *permutationally equivalent* for \mathbf{x} and \mathbf{y} if for all pairs of permutations π and π' , $r(\mathbf{x}, \mathbf{y}_\pi) \leq r(\mathbf{x}, \mathbf{y}_{\pi'})$ if and only if $s(\mathbf{x}, \mathbf{y}_\pi) \leq s(\mathbf{x}, \mathbf{y}_{\pi'})$.

The permutationally equivalent property for r has been variously presented for the t statistic for linear regression and equal-variance two-sample t -testing (including our two-sample problem) in Gatti et al. [5]. The one-to-one relationship between r and the contingency table linear trend statistic for two-way tables, which includes the Cochran-Armitage z -statistic and the 2×2 chi-square statistic, is detailed in Stokes and Koch [12] P.99, and also see Andres [3]. These relationships also hold unconditionally, i.e. they are not restricted to fixed \mathbf{x} and \mathbf{y} .

The common rank-based procedures include the Spearman correlation coefficient, which is well-known to be identical to the Pearson sample correlation (i.e. r), computed on $\text{rank}(\mathbf{x})$ and $\text{rank}(\mathbf{y})$. Similarly, the Wilcoxon rank-sum statistic is equivalent to the two-sample mean difference of ranks, as the total sum of ranks is fixed. Thus the permutationally equivalent property follows directly from the definition of r , by computing the correlation on new variables $\mathbf{x}' = \text{rank}(\mathbf{x})$, $\mathbf{y}' = \text{rank}(\mathbf{y})$.

The relationships described below depend on observed moments of \mathbf{x} or \mathbf{y} , and may not hold unconditionally for random X and Y . However, under permutation these moments remain fixed, and thus do not violate the permutationally equivalent property. Directional p -values for Fisher's exact test for 2×2 tables are determined entirely by the cell count in an arbitrarily chosen cell, after conditioning on the margins, and it is evident that the p -values are one-to-one with the cell count. Suppose without loss of generality that \mathbf{x} and \mathbf{y} are represented by binary $\{0, 1\}$ values, and we focus on the cell for which $\mathbf{x} = 1, \mathbf{y} = 1$. Then that cell count is $r = \sum x_j y_j$, proving the relation.

For the remaining “standard” statistics, such as those based on likelihood ratios, the statistic measures departure from the null in either direction, and may not be one-to-one with r^2 . The one-to-one relationship with r_Π is claimed only for separate consideration of permutations with $\text{sign}(r) < 0$ and permutations with $\text{sign}(r) > 0$. For a generalized linear model, we define $\mu_j = E[Y_j]$, with link function $g(\mu_j) = \eta_j = \beta_0 + \beta_1 x_j$. For notational convenience we define $z_{j0} = 1$ and $z_{j1} = x_j$, so $\eta_j = \sum_g \beta_g z_{jg}$, for $g \in \{0, 1\}$. For any standard link function (McCullagh and Nelder [9] P30), μ_j is monotone with η_j . For the link functions of most common interest, including identity, log, logit, and probit models, the relationship is strictly increasing, and the arguments below pertain to this situation. Decreasing canonical link functions apply to exponential, gamma, and inverse Gaussian data, for which the $r, \hat{\beta}_1$ relationship in the arguments below simply needs to be reversed.

Without loss of generality, we assume that \mathbf{x} and \mathbf{y} have been scaled so that the correlation function $r(\mathbf{x}, \mathbf{y}) = \sum_j x_j y_j$. We begin by claiming that, if a unique maximum likelihood estimate exists, then the m.l.e. $\hat{\beta}_1$ and $r(\mathbf{x}, \mathbf{y})$ have the same sign. Using notation from Agresti Agresti [1], the score function is

$$\frac{\partial L_j}{\partial \beta_g} = \frac{(y_j - \mu_j) z_{jg}}{\text{var}(Y_j)} \frac{\partial \mu_j}{\partial \eta_j} \quad (2.1)$$

$$(2.2)$$

with known $\text{var}(Y_j) = \frac{\partial \mu_j}{\partial \eta_j} a(\phi)$ and dispersion parameter $a(\phi)$, so that $\frac{\partial L_j}{\partial \beta_g} = (y_j - \mu_j) z_{jg} / a(\phi)$. Careful examination of the score function shows that for nonzero x_j it is always decreasing in β_1 , regardless of β_0 . This fact may be seen by separate consideration of the four combinations of $\{\mu_j < 0, \mu_j > 0\} \times \{x_j < 0, x_j > 0\}$. Now suppose that $r(\mathbf{x}, \mathbf{y}) > 0$. The score function at $\beta_1 = 0$ is equal to $\sum_{j=1}^n \frac{(y_j - \mu_j) x_j}{\text{var}(Y_j)} \frac{\partial \mu_j}{\partial \eta_j} \propto r(\mathbf{x}, \mathbf{y}) > 0$. Therefore, the solution to the score equation must be $\hat{\beta}_1 > 0$. If $r(\mathbf{x}, \mathbf{y}) < 0$, the same reasoning implies $\hat{\beta}_1 < 0$, and so $r(\mathbf{x}, \mathbf{y})$ and $\hat{\beta}_1$ must share the same sign.

For a particular permutation π , suppose there exists another permutation π' such that $r(\mathbf{x}, \mathbf{y}_{\pi'}) > r(\mathbf{x}, \mathbf{y}_\pi) > 0$. Using $\hat{\beta}_{g,\pi}$ to denote the maximum likelihood estimates for permutation π , by the argument above,

$$L(\widehat{\beta}_{0\pi}, \widehat{\beta}_{1\pi} | \mathbf{x}, \mathbf{y}_{\pi'}) > L(\widehat{\beta}_{0\pi}, \widehat{\beta}_{1\pi} | \mathbf{x}, \mathbf{y}_\pi).$$

By the definition of maximum likelihood and the strict inequality above, it follows that

$$L(\widehat{\beta}_{0\pi'}, \widehat{\beta}_{1\pi'} | \mathbf{x}, \mathbf{y}_{\pi'}) > L(\widehat{\beta}_{0\pi}, \widehat{\beta}_{1\pi} | \mathbf{x}, \mathbf{y}_\pi).$$

Therefore the maximum loglikelihood is a monotone increasing function of the Pearson correlation coefficient over the positive range, and the same argument implies it increases with decreasing negative correlation. The null loglikelihood does not vary over permutations, so the same conclusion applies to the maximum loglikelihood ratio statistic. Note that this argument applies to the loglikelihood ratio, and not necessarily to other statistics. In particular, the logistic Wald

statistic can have aberrant behavior for extreme departures from the null Hauck and Donner [6].

3. Appendix C: Kurtosis of r_{Π}

We scale both \mathbf{x} and \mathbf{y} so that $\sum_{j=1}^n x_j = 0$, $\sum_{j=1}^n x_j^2 = 1$ and $\sum_{j=1}^n y_j = 0$, $\sum_{j=1}^n y_j^2 = 1$.

$$\begin{aligned}
 r &= \frac{(\sum x_j y_j)/(n-1) - \overline{\mathbf{x}\mathbf{y}}}{s_x s_y} \\
 &= \frac{\frac{\sum x_j y_j}{n-1}}{\sqrt{\frac{\sum_j x_j^2}{n-1} \frac{\sum_j y_j^2}{n-1}}} \\
 &= \sum_j x_j y_j
 \end{aligned} \tag{3.1}$$

We have

$$\begin{aligned}
 (\sum x_i y_i)^4 &= \sum x_i^4 y_i^4 + 4 \sum_i \sum_{j \neq i} x_i^3 x_j y_i^3 y_j + 6 \sum_i \sum_{j \neq i} x_i^2 x_j^2 y_i^2 y_j^2 \\
 &+ 12 \sum_i \sum_{j \neq i} \sum_{l \notin (i,j)} x_i^2 x_j x_l y_i^2 y_j y_l \\
 &+ \sum_i \sum_{j \neq i} \sum_{k \notin (i,j)} \sum_{m \notin (i,j,k)} x_i x_j x_k x_m y_i y_j y_k y_m
 \end{aligned} \tag{3.2}$$

We have the kurtosis of \mathbf{x} (denoted k_x and treating the vector \mathbf{x} as a “pop-

ulation”), $k_x = \frac{\sum_j \frac{x_j^4}{\frac{n}{\sum_j x_j^2}}}{(\frac{n}{\sum_j x_j^2})^2} - 3 = n \sum_j x_j^4 - 3$, so we have $\sum_j x_j^4 = \frac{k_x + 3}{n}$.

$$\begin{aligned}
E[x_j x_k^3] &= \frac{1}{n(n-1)} \sum x_j (\eta - x_j^3) \\
&= -\frac{1}{n(n-1)} \sum x_j^4 \\
&= -\frac{1}{n^2(n-1)} (k_x + 3) \\
E[x_j^3 x_k] &= \sum_j \sum_{k \neq j} x_j^3 x_k p(x_j x_k) \\
&= \frac{1}{n(n-1)} \sum_j x_j^3 (-x_j) \\
&= -\frac{1}{n(n-1)} \sum_j x_j^4 \\
&= -\frac{1}{n^2(n-1)} (k_x + 3) \\
E[x_j^2 x_k^2] &= \sum_j \sum_{k \neq j} x_j^2 x_k^2 p(x_j x_k) \\
&= \frac{1}{n-1} \sum_j x_j^2 (1 - x_j^2) \\
&= \frac{1}{n-1} - \frac{1}{n^2(n-1)} (k_x + 3) \\
E[x_j^2 x_k x_l] &= \frac{1}{n(n-1)(n-2)} \sum_j \sum_{k \neq j} \sum_{l \notin \{j, k\}} x_j^2 x_k x_l \\
&= \frac{1}{n(n-1)(n-2)} \sum_j x_j^2 \sum_{k \neq j} x_k \sum_{l \notin \{j, k\}} (-x_j - x_k) \\
&= -\frac{1}{(n-1)(n-2)} \sum_j x_j^3 \sum_{k \neq j} x_k - \frac{1}{n(n-1)(n-2)} \sum_j x_j^2 \sum_{k \neq j} x_k^2 \\
&= \frac{2}{n^2(n-1)(n-2)} (k_x + 3) - \frac{1}{n(n-1)(n-2)} \tag{3.3}
\end{aligned}$$

$$\begin{aligned}
E[x_j x_k x_l x_m] &= \frac{1}{n(n-1)(n-2)(n-3)} \sum_j \sum_{k \neq j} \sum_{l \notin (j,k)} \sum_{m \notin (l,k,j)} x_j x_k x_l x_m \\
&= \frac{1}{n(n-1)(n-2)(n-3)} \sum_j \sum_{k \neq j} \sum_{l \notin (j,k)} \sum_{m \notin (l,k,j)} x_j x_k x_l - x_j - x_k - x_l \\
&= \frac{1}{n(n-1)(n-2)(n-3)} \sum_j \sum_{k \neq j} \sum_{l \notin (j,k)} \{-x_j^2 x_k x_l - x_j x_k^2 x_l - x_j x_k x_l^2\} \\
&= \frac{1}{n(n-1)(n-2)(n-3)} \{-3(\frac{2}{n}(k_x + 3) - 1)\} \\
&= -\frac{6}{n(n-1)(n-2)(n-3)}(k_x + 3) + \frac{1}{n(n-1)(n-2)(n-3)} \quad (3.4)
\end{aligned}$$

$$\begin{aligned}
E[(\sum x_i y_i)^4] &= E[\sum x_i^4 y_i^4] + 4E[\sum_i \sum_{j \neq i} x_i^3 x_j y_i^3 y_j] + 6E[\sum_i \sum_{j \neq i} x_i^2 x_j^2 y_i^2 y_j^2] \\
&\quad + 12E[\sum_i \sum_{j \neq i} \sum_{l \notin (i,j)} x_i^2 x_j x_l y_i^2 y_j y_l] + E[\sum_i \sum_{j \neq i} \sum_{k \notin (i,j)} \sum_{m \notin (i,j,k)} x_i x_j x_k x_m y_i y_j y_k y_m] \\
&= nE[x_i^4]E[y_i^4] + 4n(n-1)E[x_i^3 x_j]E[y_i^3 y_j] + 6n(n-1)E[x_i^2 x_j^2]E[y_i^2 y_j^2] \\
&\quad + 12n(n-1)(n-2)E[x_i^2 x_j x_l]E[y_i^2 y_j y_l] \\
&\quad + n(n-1)(n-2)(n-3)E[x_i x_j x_k x_m]E[y_i y_j y_k y_m]
\end{aligned}$$

The kurtosis of r_Π is proportional to $E[(\sum x_i y_i)^4]$, and therefore can be written in terms of the linear combinations of the kurtosis of \mathbf{x} (k_x), kurtosis of \mathbf{y} (k_y), and $k_x k_y$.

4. Appendix D: Power of p_{two} vs. p_{double} .

We approximate the distribution of r_Π using a smooth density $f(r)$ (cdf F), and denote $r_\eta = F^{-1}(\eta)$, $\eta \in (0, 1)$. For fixed $\alpha < 0.5$, define r_+ as the value such that $\int_{-\infty}^{r_+} f(r)dr + \int_{r_+}^{\infty} f(r)dr = \alpha$, and we will denote $r_- = -r_+$. We assume $r_- < r_{\alpha/2}$, which further implies $r_+ < r_{1-\alpha/2}$. This assumption is essentially without loss of generality, as all of the following arguments can be applied by reversing corresponding inequalities, and in the instance of equality the two types of p -value will have equal power. It follows that $F(r_{\alpha/2}) - F(r_-) = F(r_{1-\alpha/2}) - F(r_+)$. The upper panel of Supplementary Figure 2 illustrates these critical values for a right-skewed null distribution and $\alpha = 0.05$. The red boundaries r_- , r_+ are equidistant from the mean, corresponding to rejection thresholds for p_{two} , while the green boundaries $r_{\alpha/2}$, $r_{1-\alpha/2}$ correspond to p_{double} .

We approximate the alternative density as taking the form $g(r) = \frac{1}{2}f(r - \delta) + \frac{1}{2}f(r + \delta)$ over the appropriate support, where δ determines the power. We

define the following *ordering conditions* for fixed δ :

$$F(r_{\alpha/2} - \delta) - F(r_- - \delta) > F(r_{1-\alpha/2} - \delta) - F(r_+ - \delta), \quad (4.1)$$

$$F(r_{\alpha/2} + \delta) - F(r_- + \delta) > F(r_{1-\alpha/2} + \delta) - F(r_+ + \delta). \quad (4.2)$$

Given the ordering conditions, it is simple to show that $G(r_{\alpha/2}) - G(r_-) > G(r_{1-\alpha/2}) - G(r_+)$. The left-hand side corresponds to region 1 in the lower panel of Supplementary Figure 1, which is larger than the right-hand side (region 2). Region 1 is included in the rejection region of p_{double} , while region 2 is included in the rejection region of p_{two} , and the remaining shaded regions are common to both rejection rules. Thus, the ordering conditions imply that the power of p_{double} is greater than that of p_{two} . Applying all of the above arguments when $r_- > r_{\alpha/2}$, and reversing the inequalities, again showing that the power of p_{double} is greater than that of p_{two} .

Ordering conditions for the beta approximation

Whether the ordering conditions hold depends on the precise form of f and on δ . Simulations such as shown in the main text show that for “typical” skewed densities and α values used in practice, the ordering conditions hold across a wide range of δ , and p_{double} clearly has greater power than p_{two} . Using the approximating beta density for r_{Π} with beta parameters $\alpha < \beta$ (right-skewed), we can obtain a result for extreme α and δ near zero.

For our purposes it is more convenient to work directly with the original beta random variable, rather than the rescaled version which is used to approximate r_{Π} . We will denote the random variable B , with realized value b , and null pdf and cdf $h(b)$ and $H(b)$. Recall that $r = \frac{b - E(B)}{\sqrt{\text{var}(B)(n-1)}}$, $b = r\sqrt{\text{var}(B)(n-1)} + E(B)$, and we will use b_- , etc., to refer to the values correspondingly mapped from r_- , etc. Here $E(B) = \frac{\alpha_1}{\alpha_1 + \alpha_2} < \frac{1}{2}$. p_{two} experiences an asymmetry for sufficiently small α , as the right tail extends further from the mean than the left tail. Specifically, when $\alpha \in (0, 1 - H(2E(B)))$, $b_- = 0 < b_{\alpha/2}$. Using continuity and unimodal properties of the beta density implies that $h(b_-) < h(b_{\alpha/2})$ for $\alpha \in R$, where $R = (0, \alpha')$ for some positive $\alpha' \geq 1 - H(2E(B))$. A first order Taylor expansion is $H(b + \delta) = H(b) + \delta h(b) + o(\delta)$, and we examine the second ordering condition applied to the beta random variable, by computing

$$\begin{aligned} & H(b_{\alpha/2} + \delta) - H(b_- + \delta) - \{H(b_{1-\alpha/2} + \delta) - H(b_+ + \delta)\} \\ &= \{H(b_{\alpha/2}) - H(b_-) - (H(b_{1-\alpha/2}) - H(b_+))\} \\ &+ \delta\{h(b_{\alpha/2}) - h(b_-) - (h(b_{1-\alpha/2}) - h(b_+))\} + o(\delta) \\ &= 0 + \delta\{h(b_{\alpha/2}) - h(b_-) - (h(b_{1-\alpha/2}) - h(b_+))\} + o(\delta). \end{aligned} \quad (1)$$

We have $h(b_{\alpha/2}) > h(b_-)$ and $h(b_{1-\alpha/2}) < h(b_+)$, and thus the term in braces in (1) is positive, implying that the second ordering condition holds for sufficiently small positive δ . Finally, the same argument can be applied if $\alpha_1 > \alpha_2$ (left-skewed), also showing a local power advantage for positive δ near zero.

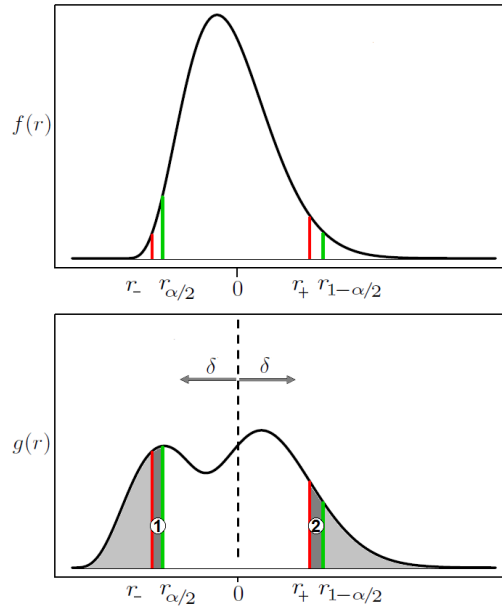


FIG 1. Illustration of the beta density approximation with $\alpha_1 = 5, \alpha_2 = 20$. The region 1 rejected by p_{double} is larger than the region 2 rejected by p_{two} .

5. Appendix E: The beta parameters α and β , in terms of skewness and kurtosis of r_Π

We use k to denote the kurtosis of r_Π , and s to denote its skewness. For parameters α and β of the beta density can be expressed analytically in terms of the kurtosis and skewness of the distribution. The skewness and kurtosis of a beta density are given in Chapter 21 of Johnson et al. [7]. Solving for α and β , the

inverse relationship is

$$\begin{aligned}
\alpha = & (3k + 36s \frac{-1}{-k^2s^2 + 32k^2 - 84ks^2 + 96k + 36s^4 - 180s^2})^{1/2} \\
& - 18s^3 \frac{-1}{-k^2s^2 + 32k^2 - 84ks^2 + 96k + 36s^4 - 180s^2})^{1/2} - 3s^2 \\
& + 3k^2s \frac{-1}{-k^2s^2 + 32k^2 - 84ks^2 + 96k + 36s^4 - 180s^2})^{1/2} \\
& - 3ks^3 \frac{-1}{-k^2s^2 + 32k^2 - 84ks^2 + 96k + 36s^4 - 180s^2})^{1/2} \\
& + 24ks \frac{-1}{-k^2s^2 + 32k^2 - 84ks^2 + 96k + 36s^4 - 180s^2})^{1/2} + 6)/(2k - 3s^2) \\
& - \frac{-6s^2 + 6k + 12}{2k - 3s^2}
\end{aligned} \tag{5.1}$$

If the above solution provides $\alpha < 0$, then we instead use

$$\begin{aligned}
\alpha = & (3k - 36s \frac{-1}{-k^2s^2 + 32k^2 - 84ks^2 + 96k + 36s^4 - 180s^2})^{1/2} \\
& + 18s^3 \frac{-1}{-k^2s^2 + 32k^2 - 84ks^2 + 96k + 36s^4 - 180s^2})^{1/2} - 3s^2 \\
& - 3k^2s \frac{-1}{-k^2s^2 + 32k^2 - 84ks^2 + 96k + 36s^4 - 180s^2})^{1/2} \\
& + 3ks^3 \frac{-1}{-k^2s^2 + 32k^2 - 84ks^2 + 96k + 36s^4 - 180s^2})^{1/2} \\
& - 24ks \frac{-1}{-k^2s^2 + 32k^2 - 84ks^2 + 96k + 36s^4 - 180s^2})^{1/2} + 6)/(2k - 3s^2) \\
& - \frac{-6s^2 + 6k + 12}{2k - 3s^2}
\end{aligned} \tag{5.2}$$

Similarly,

$$\begin{aligned}
\beta = & -(3k + 36s \frac{-1}{-k^2s^2 + 32k^2 - 84ks^2 + 96k + 36s^4 - 180s^2})^{1/2} \\
& - 18s^3 \frac{-1}{-k^2s^2 + 32k^2 - 84ks^2 + 96k + 36s^4 - 180s^2})^{1/2} \\
& - 3s^2 + 3k^2s \frac{-1}{-k^2s^2 + 32k^2 - 84ks^2 + 96k + 36s^4 - 180s^2})^{1/2} \\
& - 3ks^3 \frac{-1}{-k^2s^2 + 32k^2 - 84ks^2 + 96k + 36s^4 - 180s^2})^{1/2} \\
& + 24ks \frac{-1}{-k^2s^2 + 32k^2 - 84ks^2 + 96k + 36s^4 - 180s^2})^{1/2} + 6)/(2k - 3s^2),
\end{aligned}$$

and if the above solution is $\beta < 0$, then

$$\begin{aligned}
\beta = & -(3k - 36s \frac{-1}{-k^2s^2 + 32k^2 - 84ks^2 + 96k + 36s^4 - 180s^2})^{1/2} \\
& + 18s^3 \frac{-1}{-k^2s^2 + 32k^2 - 84ks^2 + 96k + 36s^4 - 180s^2})^{1/2} \\
& - 3s^2 - 3k^2s \frac{-1}{-k^2s^2 + 32k^2 - 84ks^2 + 96k + 36s^4 - 180s^2})^{1/2} \\
& + 3ks^3 \frac{-1}{-k^2s^2 + 32k^2 - 84ks^2 + 96k + 36s^4 - 180s^2})^{1/2} \\
& - 24ks \frac{-1}{-k^2s^2 + 32k^2 - 84ks^2 + 96k + 36s^4 - 180s^2})^{1/2} + 6)/(2k - 3s^2)
\end{aligned}$$

If both \mathbf{x} and \mathbf{y} are highly skewed, occasionally there are no real solutions for α and β , and we instead use a shifted gamma density as an approximation Zhou et al. [13], although in our experience this is a rare occurrence. For example, the approach was not needed for any of 7129 genes in the example in the next section. In this instance, the parameters of a standard gamma density are chosen to match k and s , and then the entire density is shifted to have a mean of zero. The shifted gamma density is then used as an approximation to r_{Π} , providing left- and right-tailed p -values as above.

6. Appendix F: Computational complexity

For the 36 scenarios decribed in the main text, m ranged from 1024 to 262,144, and n ranged from 512 to 4096. Elapsed time in seconds was computed using the *system.time* function in *R* for the Xeon 2.65 GHz processor. A simple regression model fit to the model $time = \beta mn + \epsilon$, with the resulting fits shown as lines in Supplementary Figure 2. The time is approximately linear on the log scale, as expected. For large m and n , the model fits well, although variations from the fit occur for smaller values.

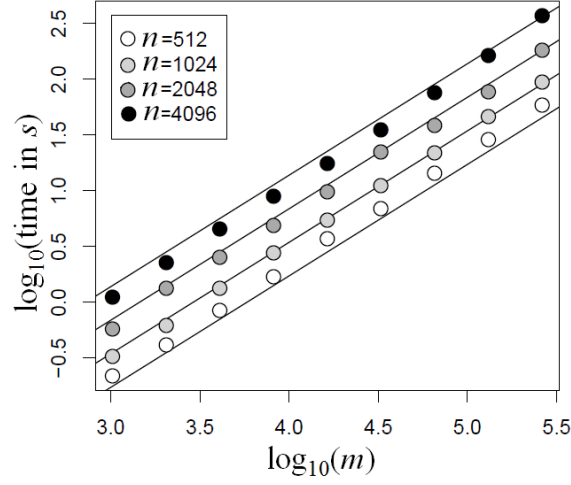


FIG 2. Elapsed time in seconds to run MCC vs. m for various values of n (axes on \log_{10} scale). Lines indicate fits from regression modeling.

7. Appendix G: Derivation of the MCC_1 terms

For a given permutation π , denote the first chosen \mathbf{y} value as $y_{\pi[1]}$. Then

$$\begin{aligned} r_{\pi} &= \sum_j x_j y_{\pi[j]} \\ &= x_1 y_{\pi[1]} + \sum_{j=2}^n x_j y_{\pi[j]} \end{aligned}$$

Using “ $-$ ” to represent the removal of an element, we have

$$\begin{aligned} r_{-\pi[1]} &= \text{corr}(x_{-1}, y_{-\pi[1]}) \\ &= \frac{(\sum_{j=2}^n x_j y_{\pi[j]})(n-1) - \sum_{j=2}^n x_j \sum_{j=2}^n y_{\pi[j]}}{\sqrt{n \sum_{j=2}^n x_j^2 - (\sum_{j=2}^n x_j)^2} \sqrt{n \sum_{j=2}^n y_{\pi[j]}^2 - (\sum_{j=2}^n y_{\pi[j]})^2}} \\ &= \frac{(\sum_{j=2}^n x_j y_{\pi[j]})(n-1) - (-x_1)(-y_{\pi[1]})}{\sqrt{n(1-x_1^2) - (-x_1)^2} \sqrt{n(1-y_{\pi[1]}^2) - (-y_{\pi[1]})^2}} \end{aligned}$$

Rearranging terms provides

$$r_{\pi} = x_1 y_{\pi[1]} + b_{0,\pi[1]} + b_{1,\pi[1]} r_{-\pi[1]},$$

where

$$b_{0,\pi[1]} = (\sqrt{n(1-x_1^2) - (-x_1)^2} \sqrt{n(1-y_{\pi[1]}^2) - (-y_{\pi[1]})^2}) (-x_1)(-y_{\pi[1]}),$$

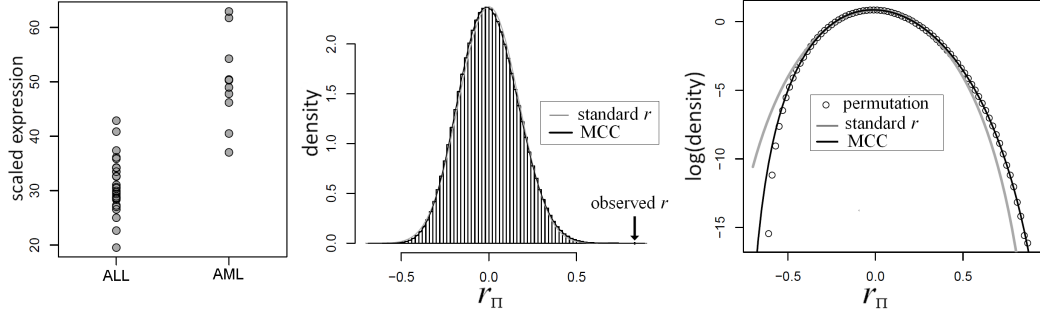


FIG 3. Expression of *LCTS4* vs. AML/ALL status, Golub dataset. The data (left panel) show a large mean difference between the leukemia types. Middle panel: the permuted correlation coefficient between \mathbf{x} and \mathbf{y} , with the overlaid standard and MCC density approximations appearing almost identical. Right panel: the histogram values on the log scale better highlight the contrast between parametric analysis (two-sample t) and permutation, which is closely matched by the MCC approximation.

$$b_{1,\pi[1]} = (\sqrt{n(1-x_1^2)} - (-x_1)^2 \sqrt{n(1-y_{\pi[1]}^2)} - (-y_{\pi[1]})^2)(n-1).$$

8. Appendix H: Example from the Golub data

We further illustrate the concepts with an example from the highly cited Golub ALL/AML expression dataset (R/ Bioconductor *golubEsets*, data signed square root transformed). The data represent expression of $m = 7129$ genes for $n = 38$ samples, 27 of which are from patients with Acute Lymphoblastoid Leukemia, and 11 from patients with Acute Myeloid Leukemia. Differential expression analysis of AML/ALL status by equal-variance t -tests reveals that the gene *LCTS4* shows the most evidence, with $p = 9.6 \times 10^{-11}$. Here \mathbf{x} is the gene's expression, and \mathbf{y} is a $\{0, 1\}$ indicator vector for AML status. Other parametric tests provide wildly differing evidence (8 orders of magnitude), with $p = 3.0 \times 10^{-6}$ for an unequal variance t -test, and $p = 8.6 \times 10^{-3}$ for a logistic regression of ALL/AML status on the gene's expression. These differences result in different qualitative conclusions – for example, a Bonferroni multiple-test correction applied to the equal variance t results in $p_{\text{Bonferroni}} = 6.8 \times 10^{-7}$, while for logistic regression is $p_{\text{Bonferroni}} = 1$.

Supplementary Figure 3 shows the results for this gene. For much of the range, the histogram is closely approximated by the standard r density, the difference between standard r and MCC is almost imperceptible. However, the standard density fails in the extremes, as can be seen on the log scale in the figure, while the MCC approach continues to work well in the extremes. For this gene, we performed 2×10^9 permutations, determining $p_{\text{double}} = 2.3 \times 10^8$ and $p_{\text{two}} = 1.1 \times 10^8$, while MCC gives estimates of $p_{\text{double}} = 2.1 \times 10^8$ and $p_{\text{two}} = 1.1 \times 10^8$.

We note that the standard density approximation is intended for uncondi-

tional inference, i.e. not conditioning on the observed \mathbf{x} and \mathbf{y} . Thus it is in some sense unfair to expect a close correspondence to the permutation distribution, which is inherently conditional on the data. However, as we show below, if the densities of X and Y are skewed, standard parametric p -values tend to be inaccurate *on average*, in a manner that is largely reflected in comparisons such as shown in Figure 3.

9. Appendix I: Additional saddlepoint comparisons

A well-studied example facilitates comparison to competing methods of permutation approximation. The two-sample dataset ($n = 16$) analyzing the effect of drugs on pain was described in Lehmann (Lehmann [8]) was further analyzed by Robinson [11] and Booth and Butler [4] to demonstrate saddlepoint methods as an alternative to permutation. The published results include tests and confidence intervals using exact methods (originally based on 100,000 permutations, improved here to 10^8 permutations), saddlepoint and Edgeworth expansions, to which we add our MCC results (Supplementary Table 1). The MCC approach is highly accurate, performing as well or better than the competing approximations, and is easier to implement.

TABLE 1
Hours of pain relief due to drugs, treatment A vs. treatment B. Data originally from Lehmann (1975, p. 37)

A: 6.8, 3.1, 5.8, 4.5, 3.3, 4.7, 4.2, 4.9;
B: 4.4, 2.5, 2.8, 2.1, 6.6, 0.0, 4.8, 2.3.

<i>pval/Sign. Level</i>	<i>Exact^a</i>	<i>Exact^b</i>	<i>Skovgaard1^c</i>	
	0.102	0.101	0.097	0.089
0.991	(−1, 3.97)	(−1.03, 3.98)		(−0.96, 3.88)
0.975	(0.62, 3.53)	(−0.62, 3.57)		(−0.57, 3.5)
0.95	(−0.3, 3.26)	(−0.32, 3.26)	(−0.30, 3.26)	(−0.27, 3.22)
<i>pval/Sign. Level</i>	<i>Robinson2^a</i>	<i>Edgeworth^a</i>	MCC	MCC ₁
	0.101	0.098	0.101	0.098
0.991	(−1.04, 3.95)	(−0.93, 3.87)	(−1.03, 3.98)	(−1.03, 3.98)
0.975	(−0.64, 3.56)	(−0.57, 3.51)	(−0.61, 3.56)	(−0.61, 3.56)
0.95	(−0.33, 3.28)	(−0.29, 3.23)	(−0.31, 3.26)	(−0.31, 3.26)

a From Robinson(1982);

b Our more refined exact value based on 10^8 permutations;

c The Skovgaard p-value and confidence interval repeated from Booth and Butler [4].

As another example, Supplementary Table 2 show the results for the second two-sample dataset, originally from Lehmann (Lehmann [8]) and further analyzed by Robinson [11] to demonstrate saddlepoint methods as an alternative to permutation. The published results include tests and confidence intervals using exact methods (originally based on 100,000 permutations), saddlepoint and Edgeworth expansions, to which we add more precise exact calculations and our MCC results. The MCC approach is highly accurate, performing as well or better than the competing approximations.

TABLE 2
Robinson table 2

Data for Robinson Table2:
Effect of analgesia for two classes. Data originally from Lehmann (1975, p 92)
Class I: 17.9,13.3,10.6,7.6,5.7,5.6,5.4,3.3,3.1,0.9
Class II: 7.7,5.0,1.7,0.0,-3.0,-3.1,-10.5.

Sign. Level	<i>Exact</i> ^a	<i>Exact</i> ^b	<i>Skovgaard1</i> ^c	<i>Robinson1</i> ^a
0.990	0.012 (−0.10, 16.13)	0.011 (−0.14, 15.97)	0.011	0.010 (0.06, 15.96)
0.975	(0.92, 14.68)	(0.96, 14.61)		(1.18, 14.51)
0.95	(1.88, 13.52)	(1.88, 13.52)		(2.07, 13.46)
	<i>Robinson2</i> ^a	<i>Edgeworth</i> ^a	MCC	MCC ₁
	0.011 (−0.15, 16.19)	0.014 (−0.02, 15.76)	0.011 (−0.16, 15.39)	0.096 (−0.16, 15.40)
	(0.98, 14.72)	(1.07, 14.44)	(0.96, 14.29)	(0.96, 14.31)
	(1.86, 13.64)	(1.95, 13.45)	(1.88, 13.40)	(1.88, 13.41)

^a From Robinson(1982); ^b Our more refined exact value based on 10^8 permutations; ^c The Skovgaard p-value and 95% CI as repeated in Booth and Butler [4].

10. Appendix J: Derivation of the moments of stratified $A = \sum A_k$

Here we propose an approximation to exact testing in which permutation is performed within each stratum level for covariate \mathbf{z} .

Suppose we have K strata for \mathbf{z} . Let J_k denote the n_k samples belonging to stratum k . Also, define $A_k = \sum_{j \in J_k} x_j y_j$ and $A = \sum_j x_j y_j = \sum_k A_k$.

Without loss of generality, we can center the y values within each stratum, so that $\sum_{j \in I} y_j = 0$. This implies $E_\Pi(A) = 0$, which simplifies analysis. We need to solve for the first four moments of A under permutation, i.e., $E_\Pi(A^2)$, $E_\Pi(A^3)$, $E_\Pi(A^4)$, and note that the $\{A_k\}$ are independent of each other. Thus we must obtain $E_\Pi(A_k^2)$, $E_\Pi(A_k^3)$, $E_\Pi(A_k^4)$ for each k . After obtaining these moments, we can find $E_\Pi(A^2)$, etc., following standard rules for independent random variables. Similar to Appendix C, ultimately we need only compute moments for \mathbf{x} and \mathbf{y} separately. However, here \mathbf{x} and \mathbf{y} are not scaled, and so we re-derive the needed quantities.

$$(\sum x_i)^4 = \sum x_i^4 + 4 \sum_i \sum_{j \neq i} x_i^3 x_j + 6 \sum_i \sum_{j \neq i} x_i^2 x_j^2 \quad (10.1)$$

$$+ 12 \sum_i \sum_{j \neq i} \sum_{k \neq i, k \neq j} x_i^2 x_j x_k + \sum_i \sum_{j \neq i} \sum_{k \neq i, j} \sum_{l \neq i, j, k} x_i x_j x_k x_l \quad (10.2)$$

$$(\sum x_i)^3 = \sum x_i^3 + 3 \sum_i \sum_{j \neq i} x_i^2 x_j + \sum_i \sum_{j \neq i} \sum_{k \neq i, k \neq j} x_i x_j x_k$$

$$\sum_i \sum_{j \neq i} x_i^3 x_j = \sum_i \sum_j x_i^3 x_j - \sum_i x_i^4 \quad (10.3)$$

$$= (\sum x_i^3)(\sum x_j) - \sum x_i^4$$

$$\sum_i \sum_{j \neq i} x_i^2 x_j^2 = \sum_i \sum_j x_i^2 x_j^2 - \sum_i x_i^4$$

$$= (\sum x_i^2)(\sum x_j^2) - \sum x_i^4 \quad (10.4)$$

$$E(x_i^3) = \sum x_i^3 / n$$

$$\sum_i \sum_{j \neq i} \sum_{k \neq i, j} x_i^2 x_j x_k = \sum_i \sum_j \sum_k x_i^2 x_j x_k - \sum_i x_i^4 - (10.3) - 2(10.4)$$

$$= \sum_i x_i^2 (\sum x_j)^2 - \sum_i x_i^4 - (10.3) - 2(10.4)$$

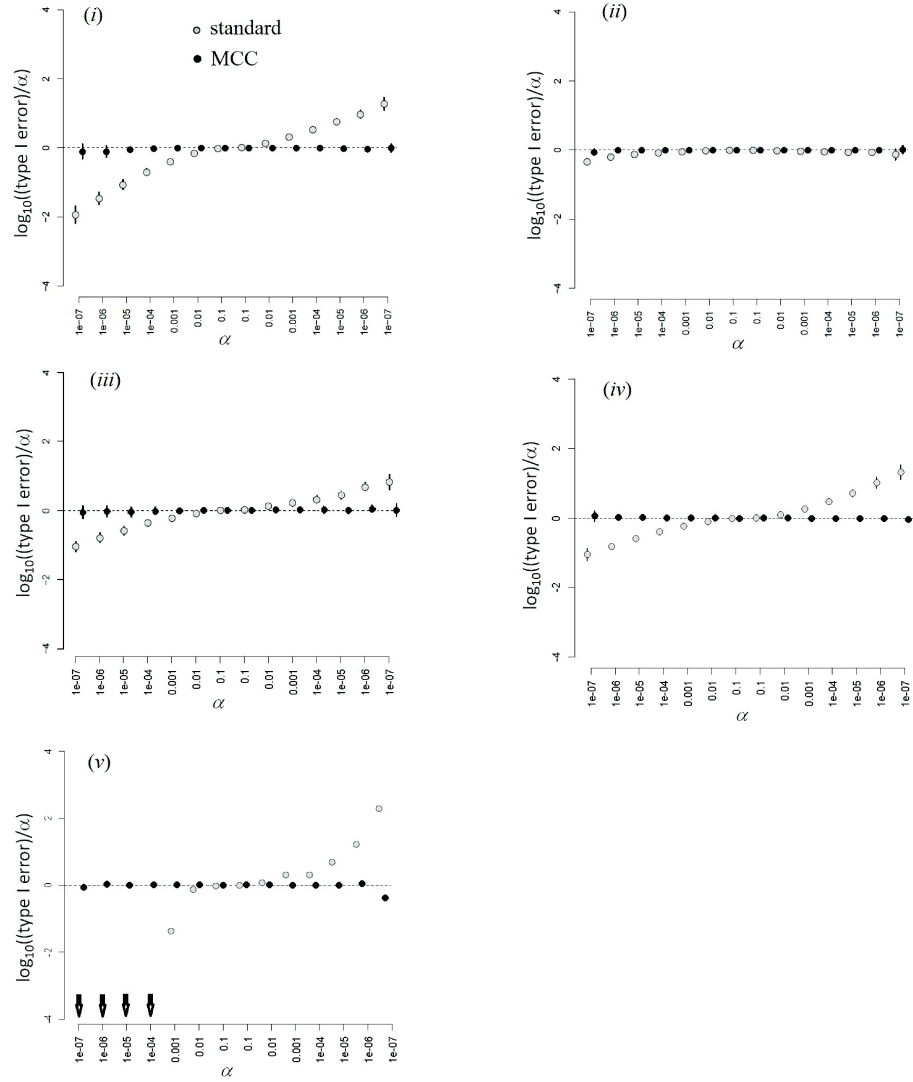
$$\begin{aligned}
E(x_i^2 x_j | i \neq j) &= \frac{\sum_i \sum_{j \neq i} x_i^2 x_j}{n(n-1)} \\
&= \frac{\sum_i \sum_j x_i^2 x_j - \sum_i x_i^3}{n(n-1)} \\
&= \frac{\sum_i x_i^2 (\sum_j x_j) - \sum_i x_i^3}{n(n-1)} \\
&= \frac{\sum_i x_i^2 n\bar{x} - \sum_i x_i^3}{n(n-1)} \\
E(x_i x_j x_k | i \neq j, i \neq k, k \neq j) &= \frac{\sum_i \sum_{j \neq i} \sum_{k \neq i, k \neq j} x_i x_j x_k}{n(n-1)(n-2)} \\
&= \frac{\sum_i \sum_j \sum_k x_i x_j x_k - 3 \sum_i \sum_{j \neq i} x_i^2 x_j - \sum_i x_i^3}{n(n-1)(n-2)} \\
&= \frac{\sum_i x_i (\sum_j x_j (\sum_k x_k)) - 3(\sum_i \sum_j x_i^2 x_j) - \sum_i x_i^3}{n(n-1)(n-2)} \\
&= \frac{n^3 \bar{x}^3 - 3(\sum_i x_i^2) n\bar{x} + 2 \sum_i x_i^3}{n(n-1)(n-2)} \\
E(x_i^2 x_j x_k | i \neq j, i \neq k, k \neq j) &= \frac{\sum_i \sum_{j \neq i} \sum_{k \neq i, k \neq j} x_i^2 x_j x_k}{n(n-1)(n-2)} \\
&= \frac{1}{n(n-1)(n-2)} \{ \sum x_i^2 (\sum x_j)^2 - \sum x_i^4 - (10.3) - 2(10.4) \} \\
&= \frac{1}{n(n-1)(n-2)} \{ \sum x_i^2 (\sum x_j)^2 - 2 \sum x_i^3 \sum x_j \\
&\quad - (\sum x_i^2)^2 + 2 \sum x_i^4 \}
\end{aligned}$$

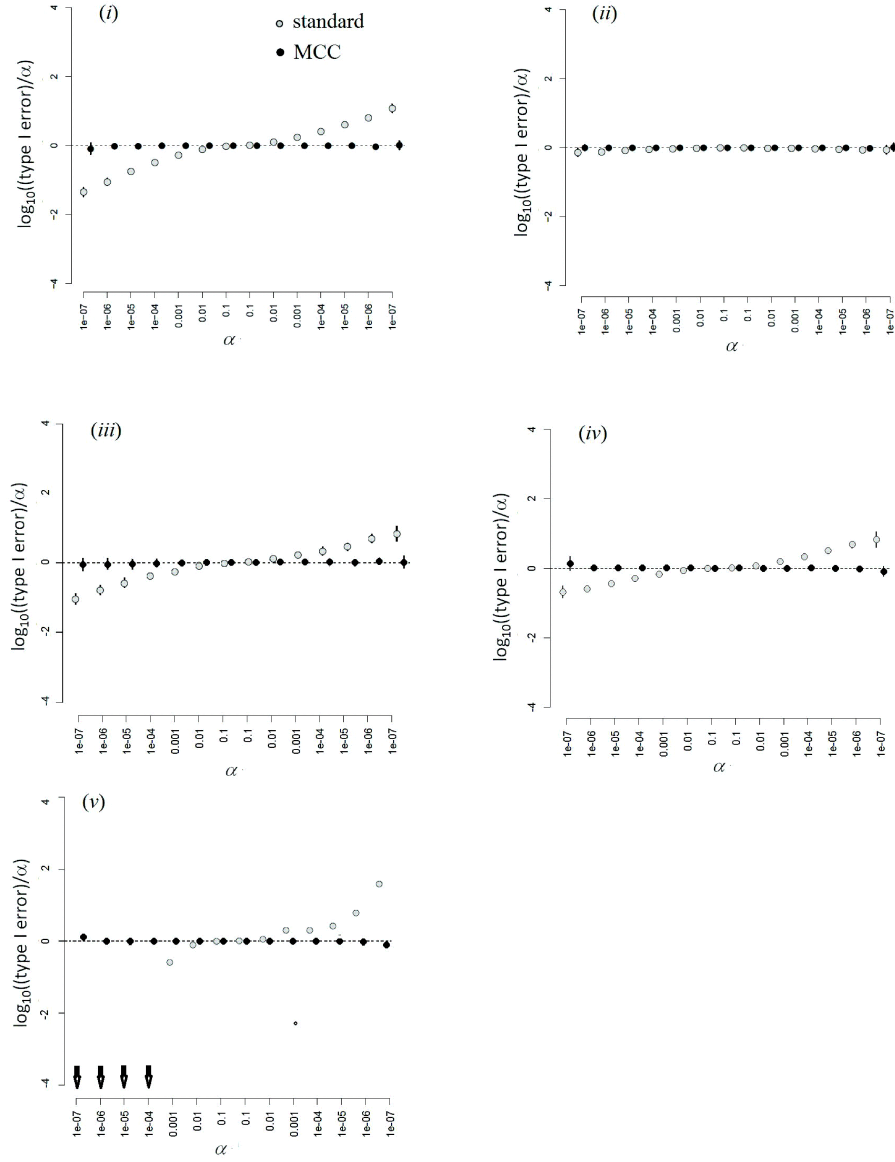
$$\begin{aligned}
(\sum xy)^4 &= \sum x^4 y^4 + \sum_i \sum_{j \neq i} x_i^3 x_j y_i^3 y_j \\
&+ \sum_i \sum_{j \neq i} x_i^2 x_j^2 y_i^2 y_j^2 + \sum_i \sum_{j \neq i} \sum_{k \neq i, k \neq j} x_i^2 x_j x_k y_i^2 y_j y_k \\
&+ \sum_i \sum_j \sum_k \sum_l x_i x_j x_k x_l y_i y_j y_k y_l
\end{aligned}$$

$$\begin{aligned}
E_{\Pi}(A_k^4) &= E[(\sum x_i y_i)^4] \\
&= \sum E(x_i^4)E(y_i^4) + \sum_i \sum_{j \neq i} E(x_i^3 x_j)E(y_i^3 y_j) \\
&+ \sum_i \sum_{j \neq i} E(x_i^2 x_j^2)E(y_i^2 y_j^2) + \sum_i \sum_{j \neq i} \sum_{k \neq i, k \neq j} E(x_i^2 x_j x_k)E(y_i^2 y_j y_k) \\
&+ \sum_i \sum_j \sum_k \sum_l E(x_i x_j x_k x_l)E(y_i y_j y_k y_l)
\end{aligned}$$

References

- [1] A. Agresti. *Categorical data analysis*, volume 359. John Wiley & Sons, 2002.
- [2] A. Agresti and B. A. Coull. Approximate is Better than “Exact for Interval Estimation of Binomial Proportions. *The American Statistician*, 52(2)(190-203), 1998.
- [3] M. Andres. Is fisher’s exact test very conservative. *Computational Statistics and Data Analysis*, 19:579–591, 1995.
- [4] J. G. Booth and R. W. Butler. Randomization distributions and saddlepoint approximations in generalized linear models. *Biometrika*, 77-4: 787–96, 1990.
- [5] D. M. Gatti, A. A. Shabalin, T. Lam, F. A. Wright, I. Rusyn, and A. B. Nobel. FastMap: fast eQTL mapping in homozygous populations. *Bioinformatics*, 25:4:482–489, 2009.
- [6] W. W. Hauck and A. Donner. Wald’s Test as Applied to Hypotheses in Logit Analysis. *Journal of the American Statistical Association*, 72:851–853, 1977.
- [7] N. L. Johnson, S. Kotz, and N. Balakrishnan. *Continuous univariate distributions, vol. 2 of wiley series in probability and mathematical statistics: Applied probability and statistics*. Wiley, New York,, 1995.
- [8] E. L. Lehmann. Nonparametrics: Statistical Methods Based on Ranks. *San Francisco: Holden-Day*, 1975.
- [9] P. McCullagh and J. A. Nelder. *Generalized Linear Model*. Chapman and Hall, 1983.
- [10] F. Pesarin and L. Salmaso. *Permutation tests for complex data: theory, applications and software*. John Wiley & Sons, 2010.
- [11] J. Robinson. Saddlepoint Approximations for Permutation Tests and Confidence Intervals. *Journal of the Royal Statistical Society*, 44(1)(91-101), 1982.
- [12] D. C. S. Stokes, M. E. and G. G. Koch. Categorical Data Analysis Using the SAS System. *SAS Institute Inc*, 2000.
- [13] Y.-H. Zhou, W. T. Barry, and F. A. Wright. Empirical pathway analysis, without permutation. *Biostatistics*, 2013.

FIG 4. Scenario (i)-(vi), sample size $n=1000$

FIG 5. Scenario (i)-(vi), sample size $n=2000$